



ORIGINAL RESEARCH COMMUNICATION

# Hemodynamic Shear Stress *via* ROS Modulates PCSK9 Expression in Human Vascular Endothelial and Smooth Muscle Cells and Along the Mouse Aorta

Zufeng Ding,<sup>1-3</sup> Shijie Liu,<sup>1</sup> Xianwei Wang,<sup>1</sup> Xiaoyan Deng,<sup>2</sup> Yubo Fan,<sup>2</sup> Changqing Sun,<sup>3</sup> Yannian Wang,<sup>3</sup> and Jawahar L. Mehta<sup>1</sup>

## Abstract

**Aims:** To investigate a possible link between hemodynamic shear stress, reactive oxygen species (ROS) generation, and proprotein convertase subtilisin/kexin type 9 (PCSK9) expression. **Results:** Using a parallel-plate flow chamber, we observed that PCSK9 expression in vascular smooth muscle cells (SMCs) and endothelial cells (ECs) reached maximal value at low shear stress (3–6 dynes/cm<sup>2</sup>), and then began to decline with an increase in shear stress. PCSK9 expression increased when cells were treated with lipopolysaccharide. PCSK9 expression was always greater in SMCs than in ECs. ROS generation followed the same pattern as PCSK9 expression. Aortic branching and aorta–iliac bifurcation regions of mouse aorta that express low shear stress were also found to have greater PCSK9 expression (*vs.* other regions). To determine a relationship between ROS and PCSK9 expression, ECs and SMCs were treated with ROS inhibitors diphenylene-iodonium chloride and apocynin, and both markedly reduced PCSK9 expression. Relationship between PCSK9 and ROS was further studied in p47<sup>phox</sup> and gp91<sup>phox</sup> knockout mice; both mice strains revealed low PCSK9 levels in serum and mRNA levels in aorta–iliac bifurcation regions (*vs.* wild-type mice). Other studies showed that ROS and NF- $\kappa$ B activation plays a bridging role in PCSK9 expression *via* lectin-like oxidized low-density lipoprotein receptor-1 (LOX-1). **Innovation:** Low shear stress induces PCSK9 expression, which is mediated by NADPH oxidase-dependent ROS production. **Conclusions:** This study provides evidence that low shear stress enhances PCSK9 expression in concert with ROS generation in vascular ECs and SMCs. ROS seem to regulate PCSK9 expression. We propose that PCSK9-ROS interaction may be important in the development of atherosclerosis in arterial channels with low shear stress. *Antioxid. Redox Signal.* 22, 760–771.

## Introduction

**H**EMODYNAMIC SHEAR STRESS determines vascular pathology such as development of atherosclerosis, aneurysms, poststenotic arterial dilatation, and arteriovenous malformations (27). Hemodynamic shear stress also regulates accumulation or uptake of native and oxidized low-density lipoprotein (oxLDL) (11). Endothelial cells (ECs) present on the luminal surface of the blood vessels are con-

stantly subjected to varying levels of hemodynamic shear stress and adapt to changes in shear stress by altering their structure and function. Smooth muscle cells (SMCs), another major component of blood vessels, are also exposed to shear stress driven by pressure gradient along the length of vascular channels. Low shear stress in the order of  $\approx 1$  dyne/cm<sup>2</sup> on arterial SMCs has been shown to affect SMC function, such as proliferation and migration (44, 45). During state of health when the EC lining is intact, exposure of SMCs to shear stress

<sup>1</sup>Central Arkansas Veterans Healthcare System and the Departments of Medicine, and Physiology and Biophysics, University of Arkansas for Medical Sciences, Little Rock, Arkansas.

<sup>2</sup>Key Laboratory for Biomechanics and Mechanobiology of Ministry of Education, School of Biological Science and Medical Engineering, Beihang University, Beijing, People's Republic of China.

<sup>3</sup>College of Public Health, Zhengzhou University, Zhengzhou, Henan, People's Republic of China.

**Innovation**

Proprotein convertase subtilisin/kexin type 9 (PCSK9) inhibition has emerged as a novel therapy to treat hypercholesterolemia. This study based on cultured vascular endothelial cells and smooth muscle cells and several mice strains provides the first evidence that low shear stress enhances PCSK9 expression in concert with reactive oxygen species (ROS) generation. ROS seem to regulate PCSK9 expression. We propose that PCSK9-ROS interaction may be important in the development of atherosclerosis in arterial channels with low shear stress.

is limited, but when EC lining is disrupted as during angioplasty or surgical endarterectomy, alterations in shear stress may directly influence SMC function. However, most studies have focused on changes in structure and function of ECs in response to changes in shear stress (12, 39), and there is paucity of data on the influence of changes in shear stress on SMCs function along the arterial channels.

Proprotein convertase subtilisin/kexin type 9 (PCSK9) is an enzyme that in humans is encoded by the *PCSK9* gene, synthesized mainly in the liver, kidney, and small intestine (1, 10, 31). This protein plays a regulatory role in cholesterol homeostasis by binding to the epidermal growth factor-like repeat A (EGF-A) domain of the low-density lipoprotein receptor (LDLr), inducing LDLr degradation (48). Inhibition

of PCSK9 drastically reduces LDL levels in serum (29). Thus, PCSK9 inhibition has emerged as a potential novel drug therapy to treat hypercholesterolemia and associated diseases such as atherosclerosis (46). Although the vast majority of the studies have focused on the role of PCSK9 in LDLr expression in liver and kidney, an increasing body of evidence suggests that *PCSK9* gene is also present in extrahepatic and extra-renal tissues (47). Inflammation induces marked changes in lipid and lipoprotein metabolism, and PCSK9 expression has been shown to be upregulated during inflammation (22). Of note, hypercholesterolemia and related vascular disease states, such as atherosclerosis, are associated with an inflammatory state (33).

We posited that there might be a link between shear stress and PCSK9 expression, particularly during inflammation. To examine this postulate, we used a parallel-plate flow chamber technique in which one can control shear stress and examine PCSK9 expression in EC and SMC monolayer cell culture. In addition, we studied distribution of PCSK9 along mice aortic segments in which there are profound variations in shear stress.

**Materials and Methods**

*Experimental shear stress system*

An experimental perfusion system as previously described by Ding *et al.* (18) was used (Fig. 1A). The system consists of

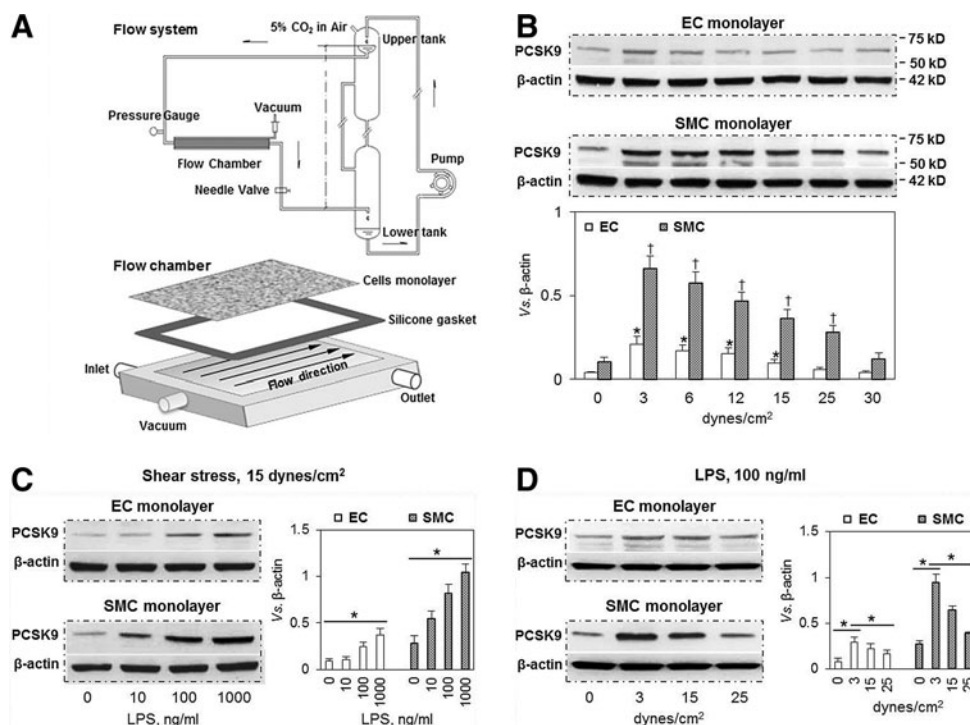


**FIG. 1. Effect of shear stress on PCSK9 expression in ECs and SMCs.** (A) Schematic drawing of the experimental flow chamber system. The overflow upper-tank provides a steady flow and pressure to ECs and SMCs. (B) Low shear stress (3–6 dynes/cm<sup>2</sup>) markedly induced PCSK9 expression, while higher shear stress had much less effect in both ECs and SMCs. At all levels of shear stress, PCSK9 expression was much higher in SMCs compared with ECs. \**p* < 0.05 compared with control in ECs, †*p* < 0.05 compared with control in SMCs. (C) At normal shear stress (15 dynes/cm<sup>2</sup>), LPS induced PCSK9 expression in a dose-dependent manner in both ECs and SMCs. Again, PCSK9 expression was much greater in SMCs compared with ECs. (D) In LPS-treated cells, low shear stress induced more PCSK9 expression in ECs and SMCs. Bar graphs represent data in mean ± SD based on five independent experiments, \**p* < 0.05. ECs, endothelial cells; PCSK9, proprotein convertase subtilisin/kexin type 9; SMCs, smooth muscle cells.

a head tank, a downstream collecting reservoir, a modified parallel-plate flow chamber with a height of  $0.5 \times 10^{-3}$  m, a peristaltic flow pump (FH100; Thermo Fisher Scientific) to circulate the perfusion fluid (cell culture medium), and a humidified atmosphere with 5% CO<sub>2</sub>. A pressure transducer and a flow meter were used to monitor the perfusion pressure and the flow rate through the flow chamber, respectively. During the experiment, the flow chamber was kept at a constant temperature of 37°C.

Wall shear stress was calculated as follows:  $\tau = 6 \mu Q / wh^2$ , where  $\mu$  is the viscosity of the medium and  $Q$  is the flow rate,  $h$  and  $w$  are the width and height of the parallel-plate flow chamber. During experimentation, wall shear stress was varied from 0 to 30 dynes/cm<sup>2</sup>, while perfusion pressure in the flow chamber was kept at 100 mmHg.

#### Cell culture

Human primary aortic ECs and SMCs were purchased from ATCC. ECs and SMCs were maintained in vascular cell basal medium with EC growth kit containing VEGF and SMC growth kit (ATCC), respectively. ECs or SMCs at three to seven passages were seeded on a glass slide with a density of  $1 \times 10^6$  cells/cm<sup>2</sup>. To form a confluent monolayer, cultured ECs and SMCs were incubated for 2 days at 37°C with 5% CO<sub>2</sub>, and then the experiments continued. The culture medium was renewed every 2 days.

#### Induction of inflammatory state

For each experiment, the height of the head-tank and the resistance of the outlet tubing were adjusted so that a chosen flow rate (and therefore, wall shear stress) through the flow chamber could be obtained. Cells were preconditioned with steady flow at a normalized arterial shear stress of 15 dynes/cm<sup>2</sup> for 24 h. To simulate an inflammatory state, ECs and SMCs were incubated with lipopolysaccharide (LPS, 1–1000 ng/ml) for another 24 h.

#### Animals

C57BL/6 background wild-type (WT), PCSK9, p47<sup>phox</sup>, and gp91<sup>phox</sup> knockout (KO) mice were purchased from Jackson Laboratory. All animals were housed in the breeding colony of our institution. All experimental procedures were performed in accordance with protocols approved by the Institutional Animal Care and Usage Committee, and conformed to the Guidelines for the Care and Use of Laboratory Animals published by the US National Institutes of Health. All male mice were used at 10 weeks of age.

#### In vivo inflammation model

To create an inflammatory state, WT and different KO mice of a similar weight were given LPS (10 mg/kg body weight, intravenously) (Sigma) or saline (control). Twenty-four hours after administration, mice were euthanized with pentobarbital sodium (80 mg/kg, i.p.). Then, the blood, aorta, and other tissues were harvested.

#### In vivo PCSK9 administration model

WT mice of a similar weight were injected with recombinant human PCSK9 protein (hPCSK9; Life Technologies)

(2 µg per mouse, intravenously) or saline (control). At the indicated time points, blood was collected from the tail vein. At 4 h after administration, mice were euthanized with pentobarbital sodium. Then, aorta and other tissues were collected.

#### PCSK9, LOX-1, p47<sup>phox</sup>, and gp91<sup>phox</sup> inhibition

To knockdown PCSK9, lectin-like oxidized low-density lipoprotein receptor-1 (LOX-1), p47<sup>phox</sup> and gp91<sup>phox</sup> gene expression, ECs and SMCs were transfected with human siRNA (directed at appropriate gene) for 24 h with siRNA transfection reagent (Santa Cruz Biotechnology). The medium was then replaced with normal culture medium, and cells were treated with 100 ng/ml LPS for another 24 h. As control, cells were transfected with sequence scrambled siRNA control (Santa Cruz Biotechnology). Cell lysates were utilized for Western blot analysis to verify efficacy of PCSK9, LOX-1, p47<sup>phox</sup>, and gp91<sup>phox</sup> knockdown by siRNA.

#### Quantitative real-time PCR analysis

Cells were lysed with TRIzol (Invitrogen), and mRNA was purified following the manufacturer's instructions. Samples were then quantified with Nanodrop (Thermo Scientific), and cDNA were obtained by retrotranscription of 1 µg RNA using the Revert Aid-H Minus First-Strand cDNA Synthesis Kit (Thermo Scientific). The quantitative real-time PCR (q-PCR) was run as follows: 50°C for 10 min, 95°C for 5 min, and then 40 cycles of 95°C for 10 s and 55°C for 30 s.

PCSK9 gene expression levels at aorta-iliac bifurcation area in WT and gene KO (gp91<sup>phox</sup> and p47<sup>phox</sup>) mice were analyzed by BioRad PrimePCR SYBR Green Assay pre-designed primer pair (Bio Rad).

Other primers used were LOX-1 forward, 5'-GCGACTCTAGGGGTCCTTTG-3', LOX-1 reverse, 5'-GTGAGT-TAGGTTTGCTTGCTCT-3'; gp91<sup>phox</sup> was analyzed by BioRad PrimePCR SYBR Green Assay pre-designed primer pair (Bio Rad); GAPDH forward, 5'-GGGTCTTGCAGT-CGTATGG-3', GAPDH reverse, 5'-ACCTCCTG TTTCT-GGGGACT-3'.

#### PCSK9 treatment

To simulate PCSK9 overexpression, ECs and SMCs were incubated with hPCSK9 (Life Technologies) (0.5, 1 and 2 µg/ml) for 24 h.

#### Western blot

Proteins from ECs and SMCs were purified with RIPA Lysis Buffer System (Santa Cruz Biotechnology), and loaded onto 12% Mini-PROTEAN<sup>®</sup> TGX<sup>™</sup> Precast Gel (Bio Rad) for electrophoresis. The size-separated proteins were then transferred to Hybond ECL Nitrocellulose Membranes (GE Healthcare). After blocking with 5% bovine serum albumin buffer for 1 h, the membranes were incubated with primary antibody at 1:1000 dilution overnight at 4°C. After washing with phosphate-buffered saline containing 0.1% Tween-20, the membrane was incubated with secondary antibody for 1 h and signal was detected with Pierce ECL Western Blotting Substrate (Thermo Scientific). Intensity quantification of the bands was obtained with Image J software and normalized to  $\beta$ -actin. Antibodies directed at PCSK9, P47<sup>phox</sup>, and gp91<sup>phox</sup> were purchased from Abcam.

### Enzyme-linked immunosorbant assay

Interleukin (IL)-1 $\beta$  and PCSK9 were measured in mice sera samples by IL-1 $\beta$  ELISA kit (BD Biosciences) or PCSK9 ELISA kit (Mouse/human; MBL International) as per the manufacturer's instructions.

### Flow cytometry measurement of cellular reactive oxygen species

Cellular total reactive oxygen species (ROS) generation was measured with DCFDA Cellular ROS Detection Assay Kit (Abcam). 2,7-dichlorofluorescein diacetate (DCFDA) is a fluorogenic dye that measures hydroxyl, peroxy, and other ROS activity within the cell. Fluorescence of DCFDA was measured on FL-1 channel with excitation wavelength at 485 nm and emission wavelength at 535 nm (FACS Vantage SE; Becton Dickinson). To confirm the results of cellular ROS generation by DCFDA fluorescence, superoxide anion production was quantified by Superoxide Detection Kit (Enzo Life Sciences) on FL-2 channel with excitation wavelength at 550 nm and emission wavelength at 620 nm. Data were recorded with the use of Flowing Software 2.0 as the "M2 percentage" fluorescence variation, which indicates the percentage of cells with enhanced superoxide anion production.

### Statistical analysis

Data from at least three independent experiments were used for statistical analysis. Results are shown as mean  $\pm$  SD. The Wilcoxon Mann-Whitney test was used to compare the means of two groups. ANOVA with Tukey's *post hoc* analysis was used when more than two groups were compared. A *p*-value < 0.05 was considered significant.

## Results

### Shear stress regulates PCSK9 expression

Malek *et al.* (38) have reported that shear stress in the arterial bed is in the range of 10–70 dynes/cm<sup>2</sup>; but it is much lower ( $\approx$  4 dynes/cm<sup>2</sup>) in regions of arterial curvatures and bifurcations, regions that are prone to development of atherosclerotic lesions. Therefore, we created shear stress states ranging from 1 to 30 dynes/cm<sup>2</sup>.

There were three major observations in our experiments (Fig. 1B, C): First, PCSK9 expression reached a maximal value at 3–6 dynes/cm<sup>2</sup>, and then began to decline with an increase in shear stress (12–30 dynes/cm<sup>2</sup>). At the highest shear stress (30 dynes/cm<sup>2</sup>), PCSK9 expression was almost same as in the static state (control). Second, LPS treatment of cells (mimicking inflammatory state) resulted in a marked increase in PCSK9 expression in both ECs and SMCs. The increase in response to LPS was concentration (10–1000 ng/ml) dependent, while shear stress was maintained at 15 dynes/cm<sup>2</sup> (Fig. 1C). Third, PCSK9 expression was much higher in SMCs than in ECs at all levels of shear stress in the absence or presence of LPS.

Since 100 ng/ml LPS gave a consistent and predictable response in terms of PCSK9 expression in both ECs and SMCs maintained at normal shear stress (15 dynes/cm<sup>2</sup>), we chose this LPS dose in subsequent experiments.

We examined PCSK9 expression in response to LPS at varying shear stress levels. As shown in Figure 1D, low shear stress (3 dynes/cm<sup>2</sup>) induced PCSK9 expression maximally, while high shear stress had a much smaller effect on PCSK9 expression. PCSK9 expression was greater in SMCs than in ECs. These observations are consistent with data shown in Figure 1B.

### Distribution of PCSK9 and VCAM-1 along the mouse aorta

Previous studies have shown that shear stress is lower at branch points (such as aorta arch branching and aorta–iliac bifurcation) than in the other regions (such as arch, thoracic aorta, and iliac arteries) (15, 41). Supplementary Figure S1A (Supplementary Data are available online at [www.liebertpub.com/ars](http://www.liebertpub.com/ars)) is a schematic diagram of different sections and shear stress pattern along the aorta. Of note, the branch points (aorta arch branching and aorta–iliac bifurcation) where shear stress is low and disturbed are prone to lipid deposition and to develop fatty streaks (15, 41). In thoracic aorta and iliac arteries, shear stress is high and blood flow is relatively steady; these phenomena might protect against atherosclerotic lipid deposition (3, 17, 36).

We measured PCSK9 expression in different regions of WT mice given saline (control) or LPS. As shown in Figure 2A, LPS induced a marked systemic inflammatory response as evident from IL-1 $\beta$  measurement in the serum samples by enzyme-linked immunosorbant assay (ELISA). PCSK9 levels in the serum also increased several fold after LPS administration (Fig. 2B).

We determined PCSK9 expression in different regions of aorta of saline- and LPS-treated mice with Western blotting. As shown in Figure 2C, PCSK9 expression in saline-treated mice was moderately, but significantly (*p* < 0.05), greater in aortic arch branching and aorta–iliac bifurcation regions than in the thoracic aorta and iliac arteries. PCSK9 expression was very pronounced in LPS-treated mice, and the differences in PCSK9 expression in different regions of aorta became quite obvious (Fig. 2C). These observations suggested that PCSK9 expression is higher in regions of low shear stress (*vs.* those with high shear stress), particularly during inflammatory state.

Vascular cell adhesion molecule-1 (VCAM-1) functions in combination with other adhesion molecules to regulate immune surveillance and inflammation. VCAM-1 is induced by cytokines, high levels of ROS, LPS, and oxLDL (13). Our study showed that, compared with areas of high shear stress, VCAM-1 expression was higher in regions of low shear stress, particularly during the inflammatory state (LPS administration) (Fig. 2D).

### Role of ROS in PCSK9 expression

Accumulating evidence suggests that ROS function as second messengers in cells that are exposed to various stress stimuli (19–21). Changes in shear stress or stretch also induce ROS generation (9). In this study, we measured cellular ROS by two different methods, and both methods revealed (Fig. 3A, B) that shear stress induced ROS production in both ECs and SMCs (more in SMCs than ECs). These changes were most marked at 3–6 dynes/cm<sup>2</sup>, and increasing shear stress from beyond 6 dynes/cm<sup>2</sup> had a less pronounced effect on

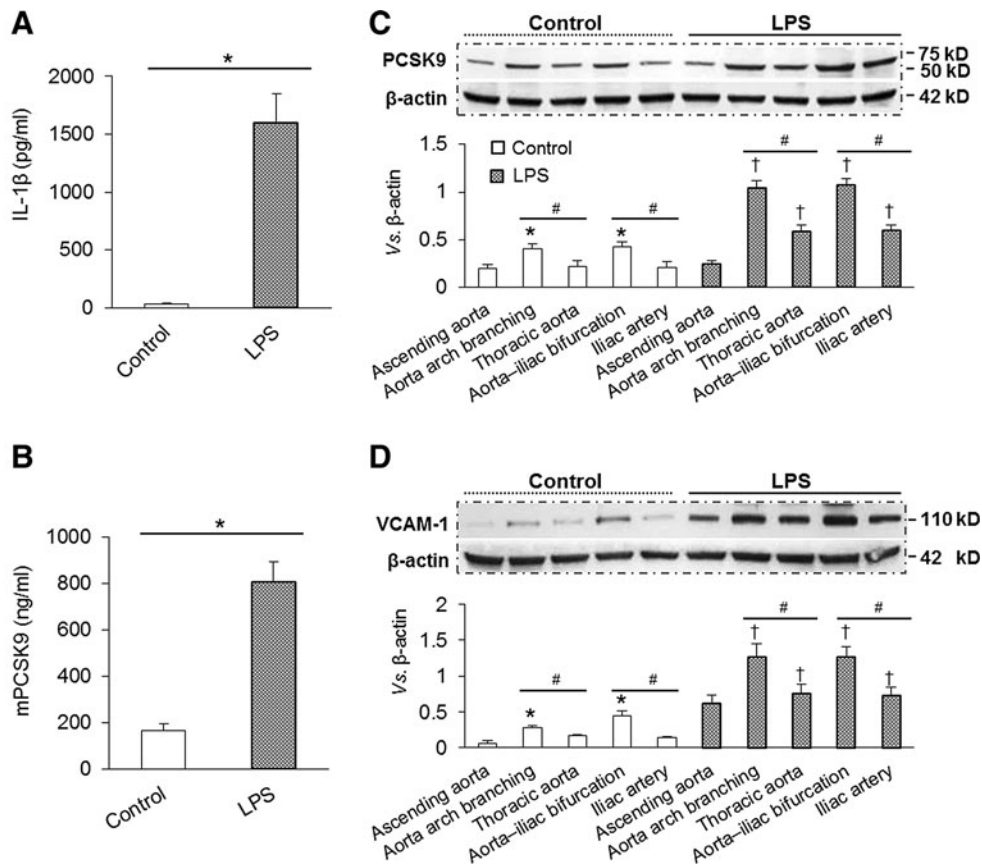


**FIG. 2. Distribution of PCSK9 and VCAM-1 along the aorta at baseline and after LPS administration.** (A) LPS administration induced a systemic pro-inflammatory state measured as IL-1 $\beta$  levels (ELISA). (B) LPS administration also induced PCSK9 release in serum measured as mPCSK9 (ELISA). (C) Representative Western blots of PCSK9 expression in saline and LPS-treated mice. PCSK9 expression was higher at the level of aortic arch branching and aorta-iliac bifurcation regions where shear stress is low and disturbed, and PCSK9 expression was much less in ascending aorta, thoracic aorta, and iliac artery where the shear stress is high and steady. (D) Representative Western blots of VCAM-1 expression along the aorta in saline and LPS-treated mice. Each aortic segment was measured in duplicate, number of mice in each group ( $n=5$ ). Bar graphs represent data in mean  $\pm$  SD, \*, #, †  $p < 0.05$ . ELISA, enzyme-linked immunosorbant assay; IL, interleukin; VCAM-1, vascular cell adhesion molecule-1.

ROS generation. The changes in ROS generation paralleled the changes in PCSK9 expression at all levels of shear stress.

Superoxide dismutase (SOD) is a major determinant of the level of cellular  $O_2^{\bullet-}$ , which enzymatically accelerates the conversion of  $O_2^{\bullet-}$  to  $H_2O_2$  and molecular oxygen. There are three isoforms of SOD, one being cytosolic copper/zinc-containing enzyme (Cu/Zn SOD). The cytosolic Cu/Zn SOD is widely distributed in the cell cytosol and nucleus, and is the primary non-mitochondrial enzyme regulating cellular  $O_2^{\bullet-}$  levels. Inoue *et al.* have reported that laminar shear stress increases Cu/Zn SOD expression in human ECs (26); we therefore measured the effect of shear stress on Cu/Zn SOD in SMCs. Our study showed that shear stress, indeed, induced Cu/Zn SOD expression in SMCs in a dose-dependent manner (Supplementary Fig. S1B).

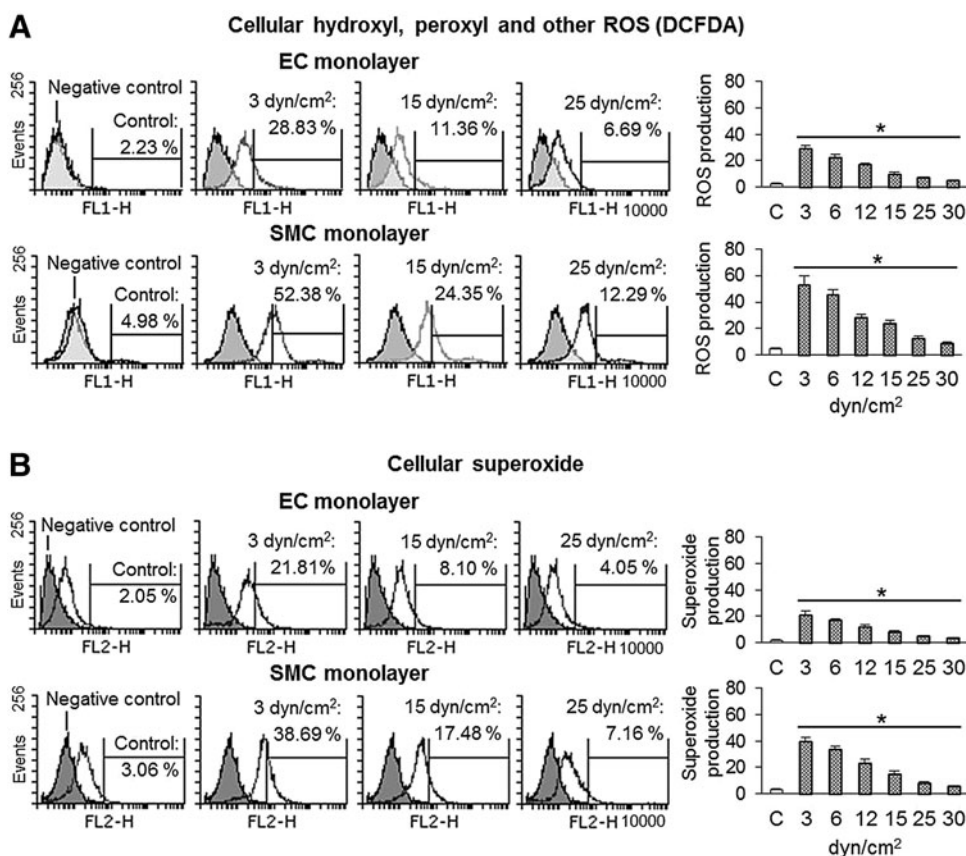
Since changes in ROS generation in ECs and SMCs paralleled PCSK9 expression, we thought that ROS may play a bridging role in shear stress-regulated PCSK9 expression. In the vasculature, several enzyme systems contribute to ROS formation, including endothelial nitric oxide (NO) synthases, respiratory chain enzymes, cytochrome P450 monooxygenases, xanthine oxidase, and NADPH oxidases. Although

all of these enzymes contribute to oxidative burden, evidence is accumulating that an initial generation of ROS by NADPH oxidases triggers the release of ROS by other enzyme systems (5, 37). Vascular NADPH oxidases have been proposed to have a role in pathological states, such as atherosclerosis (4). To determine the role of ROS in PCSK9 expression, we utilized two different inhibitors of NADPH oxidases, diphenylene-iodonium chloride (DPI) and apocynin. As shown in Figure 4A, both DPI and apocynin significantly inhibited ROS production in ECs as well as in SMCs. Importantly, pretreatment with DPI and apocynin also inhibited PCSK9 expression in ECs and SMCs, in the absence or presence of LPS (Fig. 4B).

#### PCSK9 inhibition and ROS production

Since PCSK9 expression paralleled ROS generation, we posited that there might be a bidirectional feedback between ROS production and PCSK9 expression. To test this postulate, we transfected ECs and SMCs with siRNA directed at PCSK9. As expected, PCSK9 siRNA transfection, but not the scrambled control, markedly inhibited PCSK9

**FIG. 3. Effect of shear stress on ROS production.** (A, B) Low shear stress induced ROS production in ECs and SMCs (measured by two different methods). ROS generation declined as shear stress was increased. ROS generation was greater in SMCs compared with ECs. Bar graphs represent data in mean  $\pm$  SD based on five independent experiments, \* $p$  < 0.05. ROS, reactive oxygen species.



expression (Fig. 5A). Next, we studied the effect of PCSK9 knockdown on ROS production in ECs and SMCs. As shown in Figure 5B and C, PCSK9 knockdown inhibited ROS generation in ECs and SMCs by about 30% and 50%, respectively.

To further confirm that PCSK9 inhibition attenuates ROS production, we employed mice inflammation model. ELISA showed serum levels of IL-1 $\beta$  to be increased several fold

after LPS administration in both WT and PCSK9 KO mice. Of note, the increase in IL-1 $\beta$  expression in the serum samples after LPS was much less in the PCSK9 KO than in the WT mice (Fig. 5D). PCSK9 KO also markedly inhibited the expression of NADPH oxidases p47<sup>phox</sup> and gp91<sup>phox</sup> in the aorta (Fig. 5E). Interestingly, compared with WT mice, both p47<sup>phox</sup> and gp91<sup>phox</sup> KO mice had less PCSK9 secretion in the serum in the absence or presence of LPS administration

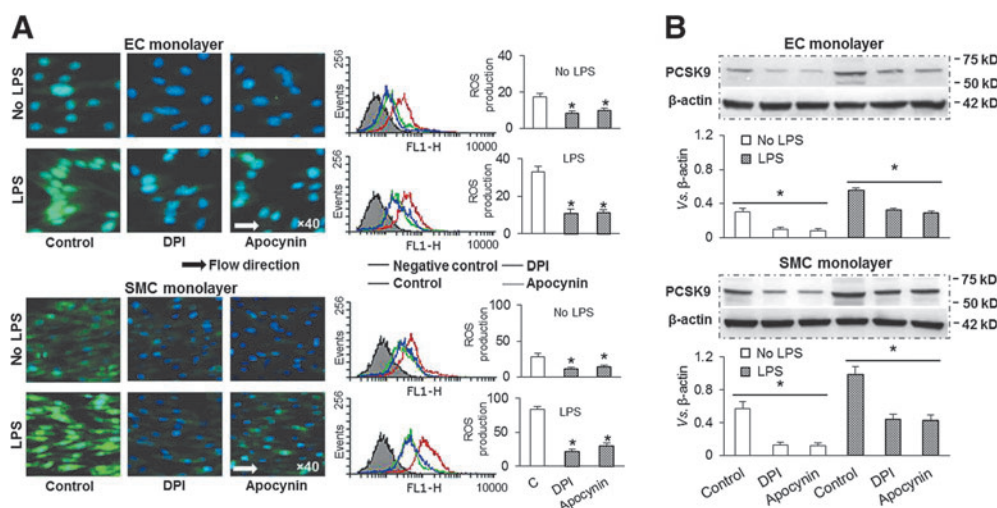


**FIG. 4. ROS inhibition and PCSK9 expression.** (A) Pretreatment with NADPH oxidase inhibitors DPI (20  $\mu$ M) or apocynin (10  $\mu$ M) markedly inhibited ROS production in both ECs and SMCs. (B) Pretreatment with DPI or apocynin also reduced PCSK9 expression in both ECs and SMCs. Both ECs and SMCs were exposed to shear stress at 15 dynes/cm<sup>2</sup>. Bar graphs represent data in mean  $\pm$  SD based on five independent experiments, \* $p$  < 0.05. DPI, diphenylene-iodonium chloride. To see this illustration in color, the reader is referred to the web version of this article at [www.liebertpub.com/ars](http://www.liebertpub.com/ars)

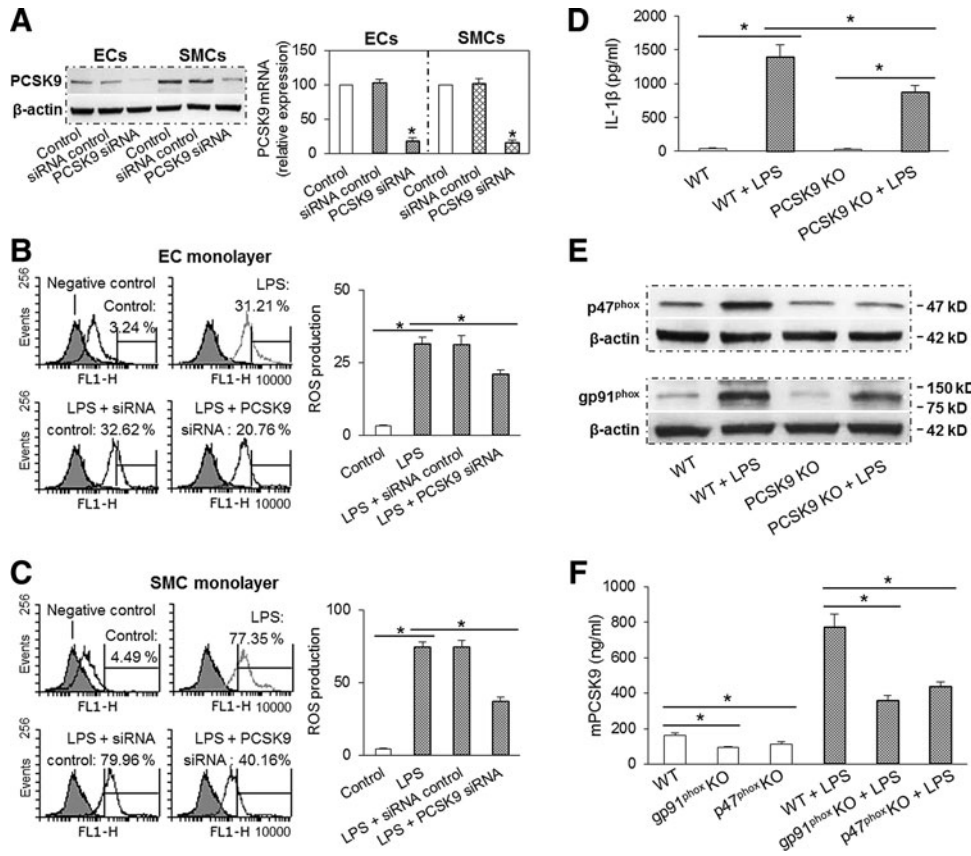


**FIG. 5. PCSK9 inhibition and ROS production.** (A) PCSK9 was significantly inhibited by its siRNA transfection in ECs and SMCs. (B, C) PCSK9 knockdown markedly inhibited ROS production in ECs and SMCs (DCFDA staining measured by flow cytometry). Both ECs and SMCs were exposed to shear stress at 15 dynes/cm<sup>2</sup>. Bar graphs represent data in mean  $\pm$  SD based on five independent experiments, \* $p$  < 0.05. (D) PCSK9 abrogation (KO mice) inhibited LPS induced IL-1 $\beta$  release in serum (measured by ELISA). (E) PCSK9 abrogation inhibited expression of NADPH oxidases subunits p47<sup>phox</sup> and gp91<sup>phox</sup> in aortic tissues. (F) p47<sup>phox</sup> and gp91<sup>phox</sup> KO mice showed significant reduction in PCSK9 secretion in serum. Each aorta or serum was measured in duplicate using 5 mice in each group ( $n$  = 5). Bar graphs represent data in mean  $\pm$  SD, \* $p$  < 0.05. DCFDA, 2,7-dichlorofluorescein diacetate; KO, knockout.

(Fig. 5F). Further, compared with WT mice, PCSK9 mRNA levels in aorta-iliac bifurcation areas were markedly inhibited in p47<sup>phox</sup> and gp91<sup>phox</sup> KO mice (Supplementary Fig. S1C).

#### PCSK9 treatment and ROS production

To confirm the suggestion that PCSK9 and ROS production regulates each other's expression, we conducted studies in ECs and SMCs treated with different concentrations of hPCSK9, as a model for overexpression. As shown in Figure 6A and B, hPCSK9-treated ECs and SMCs enhanced ROS production, and the effect of hPCSK9 on ROS generation was concentration dependent. Again, we observed that hPCSK9 induced more ROS production in SMCs than in ECs.

To further characterize the effects of acute hPCSK9 exposure on vascular ROS production *in vivo*, mice were given hPCSK9 (2  $\mu$ g per mouse). This resulted in a significant increase in serum hPCSK9 with a peak level of 825  $\pm$  163 ng/ml, which is in the physiological range (50–1000 ng/ml) (28, 31). Serum levels of hPCSK9 decreased very quickly over time as shown in Figure 6C. We studied the effect of PCSK9 administration on the expression of NADPH oxidase subunits (p47<sup>phox</sup> and gp91<sup>phox</sup>) in aortic tissues. As shown in Figure 6D and E, PCSK9 markedly enhanced the expression of p47<sup>phox</sup> and gp91<sup>phox</sup> in aortic tissues.

#### Relationship between PCSK9, LOX-1, ROS, and NF- $\kappa$ B

LOX-1 is the major endothelial receptor for oxLDL, and is thought to play a pro-atherogenic role (20). Our previous

studies showed that there is a loop interaction between LOX-1 and ROS, which is mainly regulated by the translocation of the transcription factor NF- $\kappa$ B (20). ROS are produced by the cells as a by-product of the metabolism of molecular oxygen at mitochondrial level; we therefore posited that NF- $\kappa$ B and ROS may play an important role in PCSK9 expression *via* LOX-1.

Similar to oxLDL, hPCSK9 induced LOX-1 expression in a dose-dependent manner (0.5–2  $\mu$ g/ml) in both ECs and SMCs, indicating a potential link between PCSK9 and LOX-1. Similar to ROS generation, hPCSK9 induced LOX-1 expression in SMCs than in ECs (Fig. 7A). Next, we observed that PCSK9 inhibition by siRNA transfection markedly inhibited LOX-1 and phospho-NF- $\kappa$ B p65 (p-NF- $\kappa$ B) expression in both ECs and SMCs in the presence of LPS (Fig. 7B). Subsequently, we studied the effect of LOX-1 inhibition on ROS production and expression of PCSK9 and p-NF- $\kappa$ B. As shown in Supplementary Figure S1E, both q-PCR and Western blot confirmed that LOX-1 expression was reduced by its siRNA transfection. As expected, LOX-1 knockdown inhibited ROS production and expression of PCSK9 and p-NF- $\kappa$ B in both ECs and SMCs (Fig. 7C, D). NADPH oxidase is a major source of ROS in blood vessels (27). Therefore, we used siRNA directed at NADPH oxidase subunits (p47<sup>phox</sup> and gp91<sup>phox</sup>) to study the effect of p47<sup>phox</sup> and gp91<sup>phox</sup> knockdown on the expression of LOX-1 and p-NF- $\kappa$ B. The efficacy of knockdown by siRNA was confirmed by Western blot as well as by q-PCR (Supplementary Fig. S1E, S1F). Further, knockdown of p47<sup>phox</sup> as well as gp91<sup>phox</sup> markedly inhibited the expression of LOX-1 and p-NF- $\kappa$ B in ECs and SMCs (Fig. 7E).

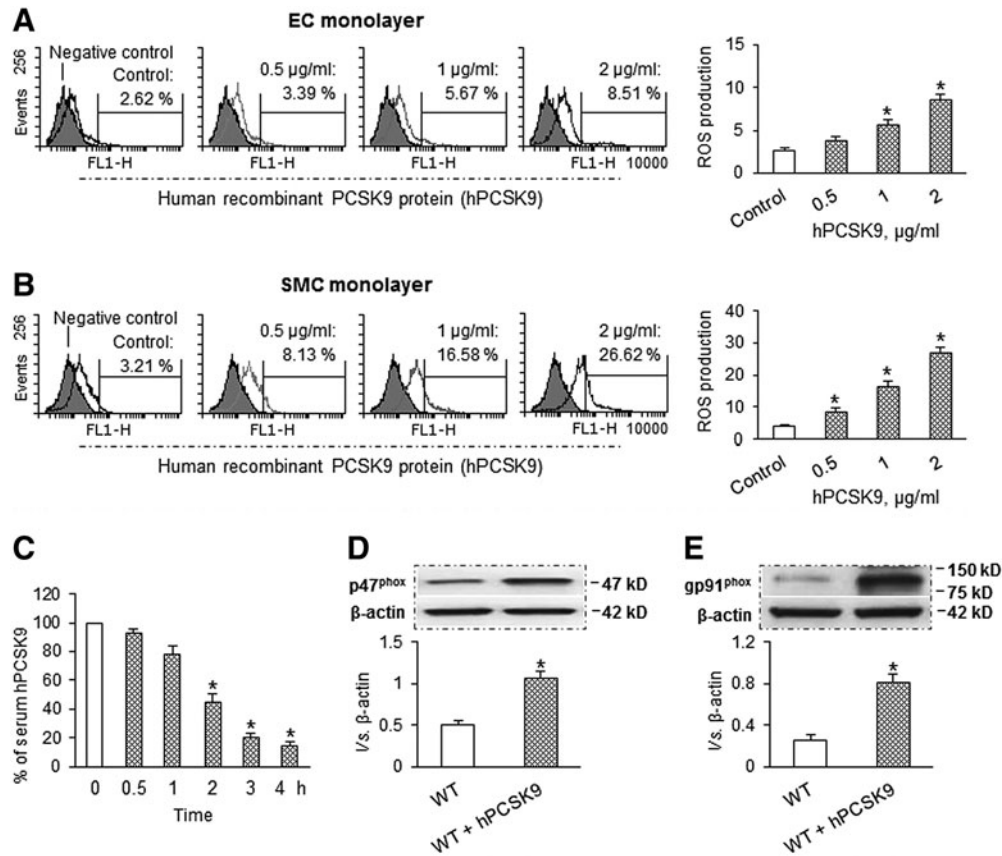


**FIG. 6. PCSK9 treatment induces ROS production.** (A, B) hPCSK9 induced ROS production in a dose-dependent manner in ECs and SMCs. Both ECs and SMCs were exposed to shear stress at 15 dynes/cm<sup>2</sup>. Bar graphs represent data in mean ± SD based on five independent experiments, \**p* < 0.05. (C) Serum levels of hPCSK9 over a 4 h period after PCSK9 administration. (D, E) Compared with WT, hPCSK9 administration increased expression of p47<sup>phox</sup> and gp91<sup>phox</sup> in aorta. Each aorta or serum was measured in duplicate using 5 mice in each group (*n* = 5). Bar graphs represent data in mean ± SD, \**p* < 0.05. hPCSK9, recombinant human PCSK9 protein.

**Discussion**

This study shows the impact of laminar shear stress on PCSK9 expression in ECs and vascular SMCs as well as in different regions of mouse aorta. Further, ROS generation also changes under the influence of shear stress, and parallels PCSK9 expression. These observations in both *in vitro* and *in vivo* settings may have important implications in lipid metabolism and atherogenesis in different vascular beds.

First, we showed in multiple settings that vascular SMCs express and secrete PCSK9 more than the ECs. Although the major sources of PCSK9 are liver, kidney, and small intestine, SMCs also excrete significant amounts of PCSK9, shown earlier by Ferri *et al.* (23), and now confirmed by us. ECs, on the other hand, secrete much smaller but significant amounts of PCSK9. The expression and release of PCSK9 by both cell types increases when the cells are exposed to LPS; however, the release by SMCs continues to be several fold greater than in ECs. In physiological states, ECs serve as a barrier to the movement of lipoproteins from the intravascular compartment to the sub-endothelium. When this barrier function of ECs is diminished, either as a consequence of loss of direct endothelial integrity (such as angioplasty and surgical endarterectomy) or as exposure to noxious stimuli (such as infections or oxidized LDL), underlying SMCs are

directly exposed to hemodynamic shear stress and blood constituents.

Second, while the alterations in EC biology in response to shear stress have been extensively studied, our observations of alterations in SMC biology in response to change in shear stress are novel and unique. We observed that low shear stress (3–6 dynes/cm<sup>2</sup>) induced a marked increase in PCSK9 expression in SMCs. Higher shear stress was associated with a gradual decline in PCSK9 expression, and the PCSK9 expression at the highest shear stress (30 dynes/cm<sup>2</sup>) was comparable to that at baseline. Qualitatively similar changes were observed in PCSK9 expression in ECs; however, SMCs exhibited significantly more PCSK9 expression than ECs at all shear stress levels. These differences persisted during inflammatory state created by treatment of cells with LPS. It is of note that PCSK9 negatively regulates LDLr expression, leading to high plasma LDL concentrations, and presumably greater LDL cholesterol deposition in the atherosclerosis-prone regions.

Arguably, atherosclerosis occurs preferentially in regions characterized by abnormal flow and shear stress (30, 42). Berk *et al.* (4) proposed that high shear stress is atheroprotective by inhibition of thrombosis and EC apoptosis, limitation of permeability and inflammatory response, and increased bioavailability of NO. Low shear



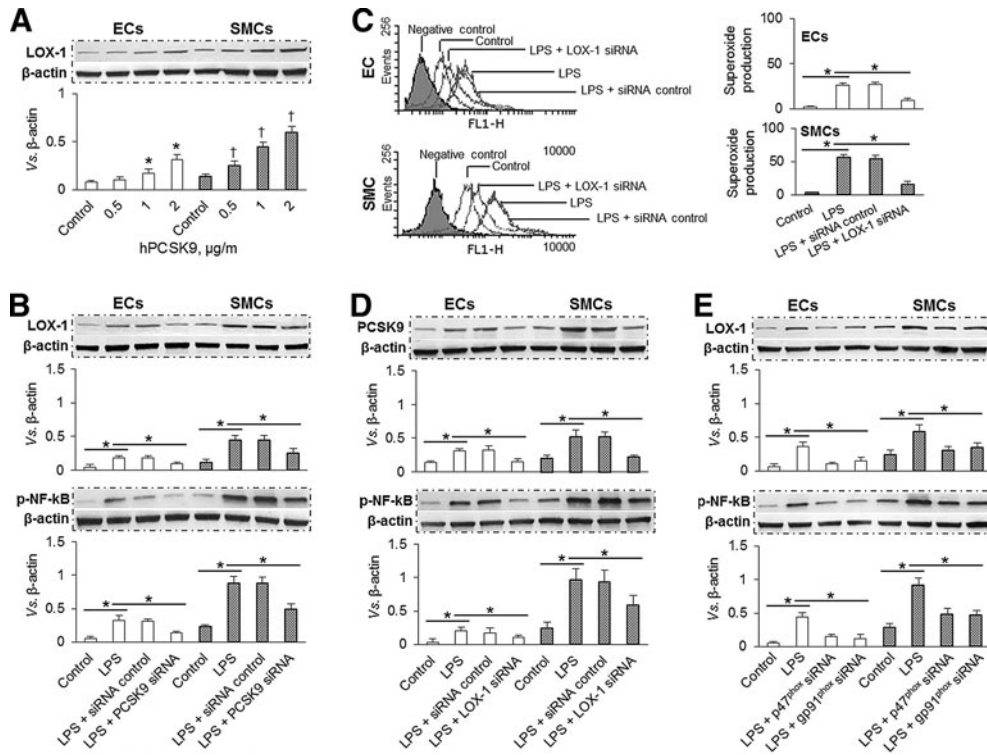


**FIG. 7. The interaction between PCSK9, LOX-1, superoxide, and NF- $\kappa$ B.** (A) hPCSK9 induced LOX-1 expression in a dose-dependent manner in ECs and SMCs. (B) PCSK9 siRNA transfection significantly inhibited expression of LOX-1 and p-NF- $\kappa$ B in ECs and SMCs. (C, D) LOX-1 siRNA transfection markedly inhibited superoxide production and expression of PCSK9 and p-NF- $\kappa$ B in ECs and SMCs. (E) Inhibition of p47<sup>phox</sup> and gp91<sup>phox</sup> by siRNA transfection significantly decreased expression of LOX-1 and p-NF- $\kappa$ B in ECs and SMCs. Both ECs and SMCs were exposed to shear stress of 15 dynes/cm<sup>2</sup>. Bar graphs represent data in mean  $\pm$  SD based on three to five independent experiments, \* $p$  < 0.05. LOX-1, lectin-like oxidized low-density lipoprotein receptor-1; p-NF- $\kappa$ B, phospho-NF- $\kappa$ B.

stress enhances ROS generation (43) and NF- $\kappa$ B activation (25, 40). Our studies showing greater PCSK9 expression in states of low shear stress provide a novel mechanism by which shear stress may regulate lipid deposition in atherosclerosis-prone regions.

We examined different regions of WT mice aorta for PCSK9 expression, and observed significantly greater PCSK9 expression in regions of low shear stress (aortic arch branching and aorta-iliac bifurcation regions) than in regions of high shear stress (thoracic aorta and iliac arteries). Although the differences between low and high shear stress regions were only modest in control animals, the differences became very pronounced during inflammatory state (administration of LPS). These results complement the *in vitro* data on PCSK9 expression in ECs and SMCs. Atherosclerosis is associated with intense inflammatory response (35), and experimental studies have shown that atherogenesis can be stimulated by inoculation of the animals with infectious agents (24, 34). Increase in PCSK9 expression, particularly during state of inflammation, may provide a plausible explanation for the development of atherosclerosis in low shear stress regions.

Fluid shear forces and vascular redox state have been proposed to be involved in the pathogenesis of lipid metabolism and atherosclerosis (6, 14, 32). De Keulenaer *et al.* (16) reported that initiation of steady laminar shear at 5 dynes/cm<sup>2</sup> resulted in a significant time-dependent increase in NADPH oxidase activity in human umbilical vein endothelial cells. Increased enzyme activity was evident as early as 1 h after exposure to steady laminar shear. However, when steady laminar shear stress was prolonged for 24 h, NADPH oxidase activity in sheared cells was not different from activity in static cells. Chin *et al.* (8) found that, compared with static

shear stress, pulsatile shear stress had a more pronounced effect on ROS generation, whereas constant high shear stress (30 dynes/cm<sup>2</sup>) had almost no effect. Consistent with these observations, we found parallel changes in ROS generation and PCSK9 expression in response to variation in shear stress. ROS generation in response to shear stress was qualitatively similar in ECs and SMCs and, not unexpectedly, increased when cells were treated with LPS. Of note, ROS generation was almost twice as much in SMCs than in ECs.

Next, we examined the relationship between ROS generation and PCSK9 expression. Using two different specific NADPH oxidases inhibitors, DPI and apocynin, we observed that both agents significantly reduced PCSK9 activation. In other experiments, PCSK9 knockdown (siRNA transfection) markedly inhibited ROS generation. Complementary to PCSK9 knockdown experiments, PCSK9 overexpression (treatment of cells with hPCSK9) increased ROS generation in a concentration-dependent manner. The definitive evidence for the positive feedback between PCSK9 and ROS generation came from experiments in PCSK9 KO and p47<sup>phox</sup> and gp91<sup>phox</sup> KO mice. The PCSK9 KO mice showed a significant suppression of NADPH oxidase (p47<sup>phox</sup> and gp91<sup>phox</sup> subunits) in aortic tissues, and p47<sup>phox</sup> and gp91<sup>phox</sup> KO mice showed almost 50% reduction in serum PCSK9 levels. Lastly, administration of exogenous hPCSK9 to WT mice resulted in a 50% increase in NADPH oxidase (p47<sup>phox</sup> and gp91<sup>phox</sup> subunits) in aortic tissues. Together, these data provide a compelling evidence for cross-talk between PCSK9 and ROS generation *via* NADPH oxidase system and indicate that fluid shear forces may have important effects on PCSK9 activation and ROS generation. NADPH oxidase family is one of the major sources for

vascular ROS production (5). Other sources such as mitochondrial electron transport enzymes, xanthine oxidase, cyclooxygenase, lipoxygenase, and uncoupled NO synthase may also affect PCSK9 secretion and participate in atherogenesis. The role of these sources of ROS generation needs further investigation.

As one of the major receptors on ECs and SMCs for oxLDL, LOX-1 is related to many pathophysiological events, including ROS generation and inflammation (11). ROS are involved in LDL oxidation; in turn, oxLDL mediates many of its biological effects by generating more intracellular ROS through binding to LOX-1. This is evidenced by the fact that anti-LOX-1 antibody markedly reduces oxLDL-induced ROS formation (7). On the other hand, LOX-1 inhibition by its antibody or siRNA transfection significantly decreases ROS generation (18, 19). NADPH oxidase is present in vascular ECs and SMCs, and it seems to be the major source of ROS production in animal models of vascular disease and in human atherosclerosis (27). In this study, we showed that ROS inhibition by siRNA transfection directed at p47<sup>phox</sup> and gp91<sup>phox</sup> markedly reduced PCSK9 expression while PCSK9 inhibition decreased LOX-1 expression in both ECs and SMCs. Further studies showed that inhibition of PCSK9, LOX-1, and ROS generation also significantly reduced p-NF- $\kappa$ B expression. Based on these findings, it is reasonable to conclude that there is an interaction between PCSK9, LOX-1, ROS, and p-NF- $\kappa$ B.

The parallel-plate flow chamber used in this study has been used by many investigators (2, 25). However, compared with the cone-and-plate device, one of the limitations of the parallel-plate flow chamber is its poor ability to exchange gases between culture medium and cells in the humidified environment. Further, it does not take into account the complex interactions between vascular cells and physiological vascular environment that exist in the living animal. For example, besides the steady laminar flow, the effect of disturbed and oscillatory flow that plays an important role in atherogenesis at bifurcation areas cannot be discerned in this system. Despite these limitations, the flow chamber studies performed by us clearly show that shear stress is a regulator of PCSK9 and it is in a large part dependent on ROS production.

Our observations based on studies in cultured vascular ECs and SMCs and several mice strains suggest that (1) shear stress is a powerful modulator of PCSK9 expression and ROS generation in ECs and SMCs, (2) SMCs are a more potent source of PCSK9 and ROS than ECs, (3) PCSK9 expression and ROS generation increase during inflammatory state, (4) there is a bidirectional cross-talk between PCSK9 and ROS generation, and (5) ROS and p-NF- $\kappa$ B may play a bridging role in LOX-1-mediated PCSK9 expression. Our preliminary observations in human tissues show increased PCSK9 expression in human atherosclerotic tissues, particularly in the SMCs (Supplementary Fig. S2).

The observations reported here may have implications in the development of atherosclerosis arterial channels with low shear stress. PCSK9 induces LDLr degradation, leading to LDL accumulation in the blood or within artery, subsequently aggravates LDL to oxLDL, which mediates many of its biological effects by generating additional intracellular ROS through binding to LOX-1.

## Acknowledgments

The authors would like to thank Dr. Jiwani Shahanawaz for providing normal and atherosclerotic human aortic sections and his expert assistance in preparing tissue slices. This work was supported by the Department of Veterans Affairs, Washington, DC, and Grants-in-Aid from the National Natural Science Foundation of China (No. 31170904, 11228205, and 61190123), Specialized Research Fund for the Doctoral Program of Higher Education of China (20121102110031).

## Author Disclosure Statement

No competing financial interests exist.

## References

1. Ai D, Chen C, Han S, Ganda A, Murphy AJ, Haeusler R, Thorp E, Accili D, Horton JD, and Tall AR. Regulation of hepatic LDL receptors by mTORC1 and PCSK9 in mice. *J Clin Invest* 122: 1262–1270, 2012.
2. Bacabac RG, Smit TH, Cowin SC, *et al.* Dynamic shear stress in parallel-plate flow chambers. *J Biomech* 38: 159–167, 2005.
3. Berceli SA, Warty VS, Sheppeck RA, Mandarino WA, Tanksale SK, and Borovetz HS. Hemodynamics and low density lipoprotein metabolism. Rates of low density lipoprotein incorporation and degradation along medial and lateral walls of the rabbit aorto-iliac bifurcation. *Arteriosclerosis* 10: 686–694, 1990.
4. Berk BC, Min W, Yan C, Surapisitchat J, Liu Y, and Hoefen R. Atheroprotective mechanisms activated by fluid shear stress in endothelial cells. *Drug News Perspect* 15: 133–139, 2002.
5. Brandes RP and Kreuzer J. Vascular NADPH oxidases: molecular mechanisms of activation. *Cardiovasc Res* 65: 16–27, 2005.
6. Brandes RP, Weissmann N, and Schröder K. Nox family NADPH oxidases in mechano-transduction: mechanisms and consequences. *Antioxid Redox Signal* 20: 887–898, 2014.
7. Chen XP, Xun KL, Wu Q, *et al.* Oxidized low density lipoprotein receptor-1 mediates oxidized low density lipoprotein-induced apoptosis in human umbilical vein endothelial cells: role of reactive oxygen species. *Vascul Pharmacol* 47: 1–9, 2007.
8. Chin LK, Yu JQ, Fu Y, Yu T, Liu AQ, and Luo KQ. Production of reactive oxygen species in endothelial cells under different pulsatile shear stresses and glucose concentrations. *Lab Chip* 11: 1856–1863, 2011.
9. Chiu JJ, Wung BS, Shyy JY, Hsieh HJ, and Wang DL. Reactive oxygen species are involved in shear stress-induced intercellular adhesion molecule-1 expression in endothelial cells. *Arterioscler Thromb Vasc Biol* 17: 3570–3577, 1997.
10. Cohen JC, Boerwinkle E, Mosley TH Jr., and Hobbs HH. Sequence variations in PCSK9, low LDL, and protection against coronary heart disease. *N Engl J Med* 354: 1264–1272, 2006.
11. Cominacini L, Pasini AF, Garbin U, *et al.* Oxidized low density lipoprotein (ox-LDL) binding to ox-LDL receptor-1 in endothelial cells induces the activation of NF- $\kappa$ B through an increased production of intracellular reactive oxygen species. *J Biol Chem* 275: 12633–12638, 2000.
12. Conway DE, Breckenridge MT, Hinde E, Gratton E, Chen CS, and Schwartz MA. Fluid shear stress on endothelial

- cells modulates mechanical tension across VE-cadherin and PECAM-1. *Curr Biol* 23: 1024–1030, 2013.
13. Cook-Mills JM, Marchese ME, and Abdala-Valencia H. Vascular cell adhesion molecule-1 expression and signaling during disease: regulation by reactive oxygen species and antioxidants. *Antioxid Redox Signal* 15: 1607–1638, 2011.
  14. Cunningham KS and Gotlieb AI. The role of shear stress in the pathogenesis of atherosclerosis. *Lab Invest* 85: 9–23, 2005.
  15. Davies PF. Hemodynamic shear stress and the endothelium in cardiovascular pathophysiology. *Nat Clin Pract Cardiovasc Med* 6: 16–26, 2009.
  16. De Keulenaer GW, Chappell DC, Ishizaka N, Nerem RM, Alexander RW, and Griendling KK. Oscillatory and steady laminar shear stress differentially affect human endothelial redox state: role of a superoxide-producing NADH oxidase. *Circ Res* 82: 1094–1101, 1998.
  17. Ding Z, Fan Y, Deng X, Sun A, and Kang H. 3,3'-Diocetadecylindocarbocyanine-low-density lipoprotein uptake and flow patterns in the rabbit aorta-iliac bifurcation under three perfusion flow conditions. *Exp Biol Med* 235: 1062–1071, 2010.
  18. Ding Z, Liu S, Sun C, Chen Z, Fan Y, Deng X, Wang X, and Mehta JL. Concentration polarization of ox-LDL activates autophagy and apoptosis via regulating LOX-1 expression. *Sci Rep* 3: 2091, 2013.
  19. Ding Z, Liu S, Wang X, Dai Y, Khaidakov M, Deng X, Fan Y, Xiang D, and Mehta JL. LOX-1, mtDNA damage, and NLRP3 inflammasome activation in macrophages: implications in atherogenesis. *Cardiovasc Res* 103: 619–628, 2014.
  20. Ding Z, Liu S, Wang X, Khaidakov M, Dai Y, and Mehta JL. Oxidant stress in mitochondrial DNA damage, autophagy and inflammation in atherosclerosis. *Sci Rep* 3: 1077, 2013.
  21. Ding Z, Wang X, Schnackenberg L, Khaidakov M, Liu S, Singla S, Dai Y, and Mehta JL. Regulation of autophagy and apoptosis in response to ox-LDL in vascular smooth muscle cells, and the modulatory effects of the microRNA hsa-let-7g. *Int J Cardiol* 168: 1378–1385, 2013.
  22. Feingold KR, Moser AH, Shigenaga JK, Patzek SM, and Grunfeld C. Inflammation stimulates the expression of PCSK9. *Biochem Biophys Res Commun* 374: 341–344, 2008.
  23. Ferri N, Tibolla G, Pirillo A, Cipollone F, Mezzetti A, Pacia S, Corsini A, and Catapano AL. Proprotein convertase subtilisin kexin type 9 (PCSK9) secreted by cultured smooth muscle cells reduces macrophages LDLR levels. *Atherosclerosis* 220: 381–386, 2012.
  24. Frishman WH and Ismail AA. Role of infection in atherosclerosis and coronary artery disease: a new therapeutic target? *Cardiol Rev* 10: 199–210, 2002.
  25. Huesa C, Helfrich MH, and Aspden RM. Parallel-plate fluid flow systems for bone cell stimulation. *J Biomech* 43: 1182–1189, 2010.
  26. Inoue N, Ramasamy S, Fukai T, Nerem RM, and Harrison DG. Shear stress modulates expression of Cu/Zn superoxide dismutase in human aortic endothelial cells. *Circ Res* 79: 32–37, 1996.
  27. Konior A, Schramm A, Czesnikiewicz-Guzik M, and Guzik TJ. NADPH oxidases in vascular pathology. *Antioxid Redox Signal* 20: 2794–2814, 2014.
  28. Konrad RJ, Troutt JS, and Cao G. Effects of currently prescribed LDL-C-lowering drugs on PCSK9 and implications for the next generation of LDL-C-lowering agents. *Lipids Health Dis* 10: 38, 2011.
  29. Kosenko T, Golder M, Leblond G, Weng W, and Lagace TA. Low density lipoprotein binds to proprotein convertase subtilisin/kexin type-9 (PCSK9) in human plasma and inhibits PCSK9-mediated low density lipoprotein receptor degradation. *J Biol Chem* 288: 8279–8288, 2013.
  30. Koskinas KC, Feldman CL, Chatzizisis YS, Coskun AU, Jonas M, Maynard C, Baker AB, Papafaklis MI, Edelman ER, and Stone PH. Natural history of experimental coronary atherosclerosis and vascular remodeling in relation to endothelial shear stress: a serial, *in vivo* intravascular ultrasound study. *Circulation* 121: 2092–2101, 2010.
  31. Lagace TA, Curtis DE, Garuti R, McNutt MC, Park SW, Prather HB, Anderson NN, Ho YK, Hammer RE, and Horton JD. Secreted PCSK9 decreases the number of LDL receptors in hepatocytes and in livers of parabiotic mice. *J Clin Invest* 116: 2995–3005, 2006.
  32. Lehoux S. Redox signalling in vascular responses to shear and stretch. *Cardiovasc Res* 71: 269–279, 2006.
  33. Libby P. Inflammation and cardiovascular disease mechanisms. *Am J Clin Nutr* 83: 456S–460S, 2006.
  34. Libby P, Egan D, and Skarlatos S. Roles of infectious agents in atherosclerosis and restenosis: an assessment of the evidence and need for future research. *Circulation* 96: 4095–4103, 1997.
  35. Libby P, Ridker PM, and Maseri A. Inflammation and atherosclerosis. *Circulation* 105: 1135–1143, 2002.
  36. Liu X, Pu F, Fan Y, Deng X, Li D, and Li S. A numerical study on the flow of blood and the transport of LDL in the human aorta: the physiological significance of the helical flow in the aortic arch. *Am J Physiol Heart Circ Physiol* 297: H163–H170, 2009.
  37. MacFarlane PM, Satriotomo I, Windelborn JA, and Mitchell GS. NADPH oxidase activity is necessary for acute intermittent hypoxia-induced phrenic long-term facilitation. *J Physiol* 587: 1931–1942, 2009.
  38. Malek AM, Alper SL, and Izumo S. Hemodynamic shear stress and its role in atherosclerosis. *JAMA* 282: 2035–2042, 1999.
  39. Mantilidewi KI, Murata Y, Mori M, Otsubo C, Kotani T, Kusakari S, Ohnishi H, and Matozaki T. Shear stress-induced redistribution of vascular endothelial-protein-tyrosine phosphatase (VE-PTP) in endothelial cells and its role in cell elongation. *J Biol Chem* 289: 6451–6461, 2014.
  40. Mohan S, Koyoma K, Thangasamy A, Nakano H, Glickman RD, and Mohan N. Low shear stress preferentially enhances IKK activity through selective sources of ROS for persistent activation of NF-kappaB in endothelial cells. *Am J Physiol Cell Physiol* 292: C362–C371, 2007.
  41. Nigro P, Abe J, and Berk BC. Flow shear stress and atherosclerosis: a matter of site specificity. *Antioxid Redox Signal* 15: 1405–1414, 2011.
  42. Peiffer V, Sherwin SJ, and Weinberg PD. Does low and oscillatory wall shear stress correlate spatially with early atherosclerosis? A systematic review. *Cardiovasc Res* 99: 242–250, 2013.
  43. Raaz U, Toh R, Maegdefessel L, Adam M, Nakagami F, Emrich FC, Spin JM, and Tsao PS. Hemodynamic regulation of reactive oxygen species: implications for vascular diseases. *Antioxid Redox Signal* 20: 914–928, 2014.
  44. Shi ZD and Tarbell JM. Fluid flow mechanotransduction in vascular smooth muscle cells and fibroblasts. *Ann Biomed Eng* 39: 1608–1619, 2011.
  45. Song S, Yamamura A, Yamamura H, *et al.* Flow shear stress enhances intracellular Ca<sup>2+</sup> signaling in pulmonary artery smooth muscle cells from patients with pulmonary arterial hypertension. *Am J Physiol Cell Physiol* 307: C373–C383, 2014.

46. Stein EA and Raal FJ. Insights into PCSK9, low-density lipoprotein receptor, and low-density lipoprotein cholesterol metabolism: of mice and man. *Circulation* 127: 2372–2374, 2013.
47. Tavori H, Fan D, Blakemore JL, Yancey PG, Ding L, Linton MF, and Fazio S. Serum proprotein convertase subtilisin/kexin type 9 and cell surface low-density lipoprotein receptor: evidence for a reciprocal regulation. *Circulation* 127: 2403–2413, 2013.
48. Zhang DW, Lagace TA, Garuti R, Zhao Z, McDonald M, Horton JD, Cohen JC, and Hobbs HH. Binding of proprotein convertase subtilisin/kexin type 9 to epidermal growth factor-like repeat A of low density lipoprotein receptor decreases receptor recycling and increases degradation. *J Biol Chem* 282: 18602–18612, 2007.

Address correspondence to:

*Dr. Jawahar L. Mehta*  
 Division of Cardiovascular Medicine  
 University of Arkansas for Medical Sciences  
 Little Rock, AR 72212

*E-mail: mehtajl@uams.edu*

*Dr. Shijie Liu*  
 Division of Physiology and Biophysics  
 University of Arkansas for Medical Sciences  
 Little Rock, AR 72205

*E-mail: sliu2@uams.edu*

Date of first submission to ARS Central, July 14, 2014; date of final revised submission, November 13, 2014; date of acceptance, December 8, 2014.

#### Abbreviations Used

DCFDA = 2,7-dichlorofluorescein diacetate  
 DPI = diphenylene-iodonium chloride  
 ECs = endothelial cells  
 EGF-A = epidermal growth factor-like repeat A  
 ELISA = enzyme-linked immunosorbant assay  
 hPCSK9 = recombinant human PCSK9 protein  
 IL = interleukin  
 KO = knockout  
 LDLr = low-density lipoprotein receptor  
 LOX-1 = lectin-like oxidized low-density lipoprotein receptor-1  
 LPS = lipopolysaccharide  
 NO = nitric oxide  
 OxLDL = oxidized low-density lipoprotein  
 PCSK9 = proprotein convertase subtilisin/kexin type 9  
 p-NF- $\kappa$ B = phospho-NF- $\kappa$ B  
 q-PCR = quantitative real-time PCR  
 ROS = reactive oxygen species  
 SMCs = smooth muscle cells  
 SOD = superoxide dismutase  
 VCAM-1 = vascular cell adhesion molecule-1  
 WT = wild type